Mini-Transplants for Chronic Myelogenous Leukemia: A Modeling Perspective

Peter S. Kim[1], Peter P. Lee[2], and Doron Levy[3]

[1] Department of Mathematics, Stanford University, Stanford, CA 94305-2125; pkim@math.stanford.edu
[2] Division of Hematology, Department of Medicine, Stanford University, Stanford, CA, 94305. ppl@stanford.edu
[3] Department of Mathematics, Stanford University, Stanford, CA 94305-2125; dlevy@math.stanford.edu

Summary. We model the immune dynamics between T cells and cancer cells in leukemia patients after a bone-marrow (or a stem-cell) transplant. We use a system of nine delay differential equations that incorporate time delays and account for the progression of cells through different stages. This model is an extension of our earlier model [1]. We conduct a sensitivity analysis of the model parameters with respect to the minimum cancer concentration attained during the first remission and the time until the first relapse. In addition, we examine the effects of varying the initial host cell concentration and the cancer cell concentration on the likelihood of a successful transplant. We observe that higher initial concentrations of general host blood cells increase the chance of success. Such higher initial concentrations can be obtained, e.g., by reducing the amount of chemotherapy that is administered prior to the transplant, a procedure known as a mini-transplant. Our results suggest that mini-transplants may be advantageous over full transplants. We identify the regions of the parameters for which mini-transplants are advantageous using statistical tools.

Key words: Chronic myelogenous leukemia, stem-cell transplant, bone-marrow transplant, non-myeloablative, mini-transplant, immune response, delay differential equations.

1 Introduction

Allogeneic bone-marrow or stem-cell transplantation (ABMT or ASCT) is currently the only known curative treatment for CML [2]. Prior to ABMT, the patient receives chemotherapy to lessen the disease and to lower the patient's immune cell population. This pre-treatment procedure is performed to reduce immune suppression by leukemia cells and to prevent graft rejection by the host.

Typically, the patient receives large doses of chemotherapy to eliminate almost all leukemia and immune cells. The treatment is called a full (or myeloablative) transplant, because the chemotherapy destroys, or ablates, nearly all the myeloid stem cells, which are the cells that produce new blood.

However, in some cases, patients cannot tolerate full chemotherapy, so they are given mini (or non-myeloablative) transplants. In mini-transplants, patients receive milder doses of chemotherapy that do not ablate the myeloid stem cells. As a result, the treatment depends more heavily on the donor immune cells to expand and destroy remaining leukemia cells.

In [1], we modeled the immune dynamics of a full transplant. Our results suggested that the expansion of donor T cells depends more on general host blood cells than on leukemia cells alone. This is because a successful transplant relies on a blood-restricted graft-versus-host disease, in which donor T cells react to antigen that is present on general host blood cells. This less discriminate reactivity results in greater proliferation of immune cells and often proves necessary, because leukemia cells usually do not provide sufficient stimulus.

In this paper we present an extension of the model of [1], in which we made two major changes: First, we assume that all target cells have two possible states: alive and dying. Dying target cells are cells that are in the process of dying due to cyotoxic interactions with T cells. These cells linger for about five minutes, during which they may still stimulate other circulating T cells. In addition, we also introduce discounting factors for cell death rates to prevents from double-counting cell deaths due to the natural decay and the cytotoxic T cell responses.

In this paper, we use the extended model to study the dynamics of mini-transplants and to determine conditions that increase the chance of a successful cure. For full and mini-transplants, chemotherapy indiscriminately kills a large number of non-leukemic host blood cells. Since these cells stimulate donor immune cells, high levels of chemotherapy might reduce the potency of the anti-leukemia immune response. In this study, we seek to understand the trade off between eliminating leukemia and host immune cells and maintaing the stimulus to donor immune cells. Under certain circumstances, we find that mini-transplants may prove more advantageous not only due to its reduced toxicity to the patient but also because it preserves a larger population of host blood cells that provide a high enough stimulation to drive the expansion of donor immune cells.

The paper is organized as follows. In Section 2, we present the state diagrams and the corresponding delay differential equations that govern the dynamics of the various cell populations. In Section 3, we present a summary of the parameter estimates that we used in the model. In Section 4, we summarize a previous result from the original paper, [1]. Then, we discuss a typical solution of the revised model and analyze the sensitivity of the revised model with respect to the parameters, using Latin Hypercube sampling. In particular, we focus on the sensitivity of the model to the initial leukemia and general

host cell concentrations. We also demonstrate that minitransplants, in which chemotherapy is administered in weaker doses, may increase the chances of a successful transplant. In Section 5, we discuss our interpretations of our results and outline future directions of study.

2 The Model

We follow our previous work [1], and track the time evolution of six cell populations. From the donor, we consider anti-cancer T cells, anti-host T cells, and all other donor cells (exclusive of the two populations explicitly mentioned). From the host, we consider cancer cells, anti-donor T cells, and general host blood cells, The anti-cancer T cells represent the cells that respond to a cancer-specific antigen and exclusively mediate the GVL effect, while the anti-host T cells represent those that respond to a general blood antigen and mediate blood-restricted GVHD. The cancer population, general donor, and general host populations can each exist in two states: alive or dying (due to previous interaction with cytotoxic T cells). This two-state formulation is a modification that is not present in [1]. As a result, our new model consists of nine delay differential equations (rather than six as in [1]).

In the following subsections we present the state diagrams and the corresponding equations for the cell populations. The various state diagrams follow the notation shown in Figure 1. The rectangles stand for the possible states for each population. The arrows represent transitions between states. The terms next to the arrows denote the rates at which cells move from one state to another. Most transitions have an associated time delay indicated by the values in the circles. The values in the circles represent the time it takes to complete the associated transition. Each circle can be thought of as a gate that holds cells in a given state until the appropriate time elapses.

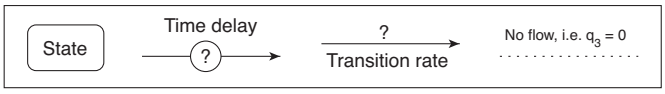

Fig. 1. The symbols used in the state diagrams

The model only explicitly measures population levels in each of the six base states, one for each cell population. Each term in the equations represents the beginning or the termination of a path connected to the base state (located at or near the center of each state diagram, denoted by the population label). The interaction initiation terms contain no delays, and the rates are proportional to the product of the two interacting populations and a mixing coefficient, k, in accordance with the law of mass action [3]. Termination terms contain each rate and delay encountered along their associated paths. Thus, the value of a given population variable, for example T_C, will at times be less than the

total number of such cells, because it will not include cells that are within the pipeline of interactions with other populations.

In [1], our model formulation allowed population levels to cross zero. This artifact required us to impose a stopping criterion that forced all populations to remain non-negative by stopping at zero rather than passing through to negative values. In the new model, presented here, the various terms in the model incorporate discounting factors that prevent the populations from crossing zero.

2.1 General Blood Cells

Figure 2(a), presents the state diagram for the alive and dying general donor blood cells, D_A and D_D. These cells provide stimulus for a graft rejection response from T_D. They play a passive role in all interactions – they do not inspect other cells.

Donor blood cells move through the state diagram as a result of interactions with T cells. Alive cells may be shifted to the dying state with probability $p_1^{T_D/D}$. (Here and throughout the paper, we denote probabilities in the form $p_i^{X/Y}$, where X represents the T cell population and Y represents the target cell population involved in the interaction. In other words, X/Y should not be interpreted as an exponent.) Also, stem cells provide a constant flow of new alive cells, and existing cells die at the natural death rate d_D.

Once a cell shifts to the dying state, D_D, it has ρ units of time to live and continue stmulating ambient T cells before death. While in this liminal dying process, cells may also die at the natural death rate d_D. Cells that have died naturally during this liminal period do not undergo a second death due to a previous cytotoxic T cell encounter ρ time units ago. Hence, we adjust the second death rate by the discounting factor $e^{-d_D\rho}$.

The alive and dying general host cells, H_A and H_D, (shown in Figure 2(b)) have an analogous role to the donor cells D_A and D_D, in that they provide stimulus for a blood-restricted GVHD response from T_H, and the population has a similar diagram and DDEs to the donor population.

T cells do not distinguish between alive and dying target cells. They are stimulated equally be both. Hence, we define the collective population variables $D = D_A + D_D$ and $H = H_A + H_D$ to denote the total donor and host cells, respectively.

The corresponding DDEs for Figures 2(a) and 2(b) are

$$\begin{aligned} \frac{dD_A}{dt} &= S_D - d_D D_A - p_1^{T_D/D} k D_A T_D, \\ \frac{dD_D}{dt} &= -d_D D_D + p_1^{T_D/D} k D_A T_D - e^{-d_D\rho} p_1^{T_D/D} k D_A(t-\rho) T_D(t-\rho) \end{aligned} \tag{1}$$

and

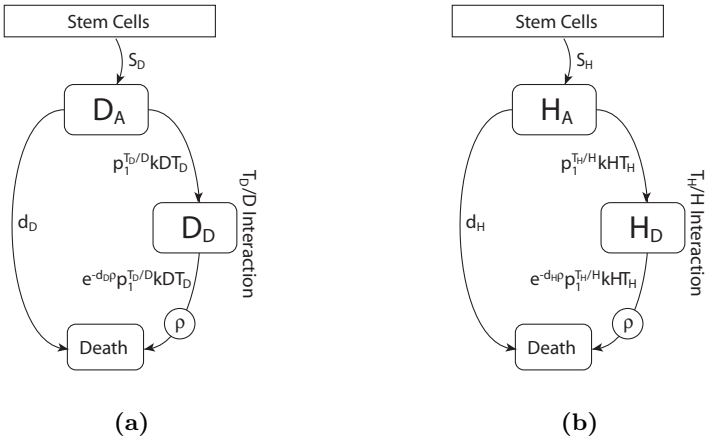

(a) **(b)**

Fig. 2. General donor and host blood cell diagrams

$$\frac{dH_A}{dt} = S_H - d_H H_A - p_1^{T_H/H} k H_A T_H, \tag{2}$$
$$\frac{dH_D}{dt} = -d_H H_D + p_1^{T_H/H} k H_A T_H - e^{-d_H \rho} p_1^{T_H/H} k H_A(t-\rho) T_H(t-\rho).$$

2.2 Anti-Cancer T Cells

Anti-Cancer T cells, T_C, interact with two other populations, the cancer cells, C, and the graft-rejecting cells T_D. The state diagram for the anti-cancer T cells is shown in Figure 3. As with the general blood cells, the cancer cells have two states, alive and dying, denoted by C_A and C_D, respectively. Also, the total cancer concentration is denoted by $C = C_A + C_D$. In the T_C/C interaction (the left wing of Figure 3) the T cells examine cancer cells and decide whether to react to the stimulus or to ignore it with probabilities $p_1^{T_C/C}$ and $p_2^{T_C/C}$, respectively. If the T cells ignore the stimulus, they return to the base state after a delay of σ, which represents the time for a nonproductive interaction. If the T cells react, they have a chance of destroying their targets through a cytotoxic response associated with a delay of ρ. After responding, the cells may enter a cycle of proliferation with probability $q_2^{T_C/C}$. Alternatively, they may forego the proliferation plan and simply recover cytotoxic capabilities (involving the replenishing of cytotoxic granulocytes) in preparation for their next encounter, returning them to the pool of active cells after a delay of υ.

We assume that T cells divide an average of n times during proliferation, resulting in 2^n times as many cells. Each cycle of division takes τ units of time to complete, hence the entire proliferation cycle requires $n\tau$ units of time. We assume that during this time, all proliferating T cells are unavailable to interact with other cells, and thus they are not included in the measure of T_C. When interacting with cancer cells, there is a probability $q_3^{T_C/C}$ that the T

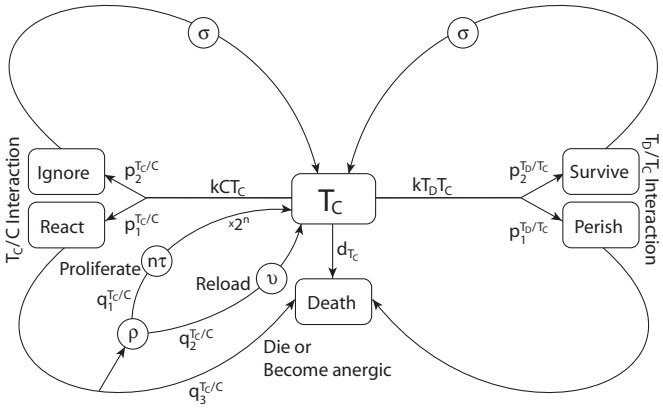

Fig. 3. Anti-cancer T cell diagram

cells will become anergic (i.e. tolerant) from the interaction. This effectively amounts to death in our simulations.

The T_D/T_C interaction (the right wing of Figure 3) represents encounters between anti-cancer cells and anti-donor T cells, where here the T_C cells are only targets. With probability $p_1^{T_D/T_C}$, the T_C cell may perish due to a graft-rejection response from T_D. In addition, some cells die at the natural rate d_{T_C}.

The DDE that corresponds to Figure 3 is:

$$\begin{aligned}\frac{dT_C}{dt} &= -d_{T_C}T_C - kCT_C - kT_DT_C + p_2^{T_C/C}kC(t-\sigma)T_C(t-\sigma)\\ &\quad + p_2^{T_D/T_C}kT_D(t-\sigma)T_C(t-\sigma)\\ &\quad + 2^n p_1^{T_C/C}q_1^{T_C/C}kC(t-\rho-n\tau)T_C(t-\rho-n\tau)\\ &\quad + p_1^{T_C/C}q_2^{T_C/C}kC(t-\rho-\upsilon)T_C(t-\rho-\upsilon).\end{aligned} \tag{3}$$

2.3 Anti-Host T Cells

Anti-host T cells, T_H, undergo interactions with all host cells C, H, and T_D. The state diagram for the anti-host T cells is given in Figure 4. In the T_H/C interaction (upper left wing of Figure 4), the anti-host T cells react with cancer in the same way as anti-cancer T cells. In other words, they can either respond to the stimulus or ignore it with probabilities $p_1^{T_H/C}$ and $p_2^{T_H/C}$, respectively. After reacting, there is a probability $q_3^{T_H/C}$ that the T cells will become anergic after the encounter with cancer cells.

In the T_H/H interaction (lower left wing of Figure 4), the T cells react in the same way with general host blood cells H, except that the general host blood cells cannot cause anergy.

In the T_H/T_D interaction (right wing of Figure 4), the two types of T cells each have a chance of killing the other. Hence, the probabilities that an anti-

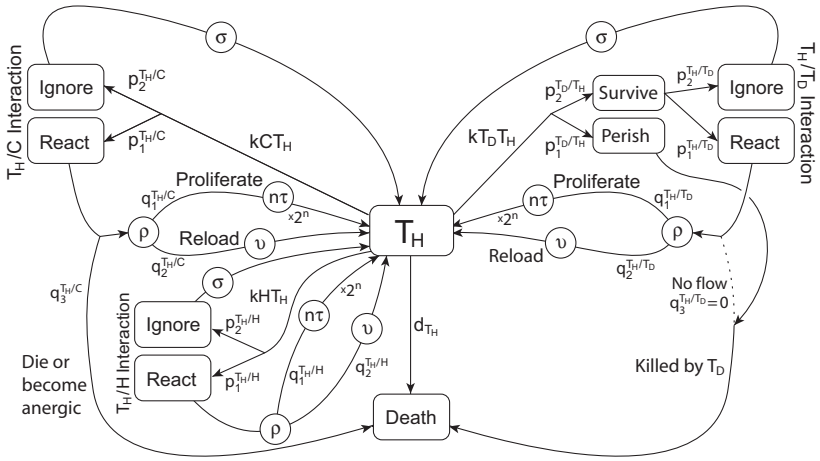

Fig. 4. Anti-host T cell diagram

host T cell survives the encounter and goes on to react to or ignore its target are $p_2^{T_D/T_H} p_1^{T_H/T_D}$ and $p_2^{T_D/T_H} p_2^{T_H/T_D}$, respectively. The extra factor of $p_2^{T_D/T_H}$ is the probability that the target anti-donor T cell does not kill the anti-host T cells. The remaining anti-host T cells get killed by their interactions with their target anti-donor T cells. Additionally, we assume that although T cells may be killed, they do not become anergic from such interactions. Hence, $q_3^{T_H/T_D} = 0$. Some cells also die at a natural death rate d_{T_H}.

The DDE that corresponds to Figure 4 is:

$$\begin{aligned}
\frac{dT_H}{dt} = & -d_{T_H} T_H - kCT_H - kT_D T_H - kHT_H \\
& + p_2^{T_H/C} kC(t-\sigma)T_H(t-\sigma) \\
& + p_2^{T_D/T_H} p_2^{T_H/T_D} kT_D(t-\sigma)T_H(t-\sigma) \\
& + p_2^{T_H/H} kH(t-\sigma)T_H(t-\sigma) \\
& + 2^n p_1^{T_H/C} q_1^{T_H/C} kC(t-\rho-n\tau)T_H(t-\rho-n\tau) \\
& + 2^n p_1^{T_H/H} q_1^{T_H/H} kH(t-\rho-n\tau)T_H(t-\rho-n\tau) \\
& + 2^n p_2^{T_D/T_H} p_1^{T_H/T_D} q_1^{T_H/T_D} kT_D(t-\rho-n\tau)T_H(t-\rho-n\tau) \\
& + p_1^{T_H/C} q_2^{T_H/C} kC(t-\rho-\upsilon)T_H(t-\rho-\upsilon) \\
& + p_1^{T_H/H} q_2^{T_H/H} kH(t-\rho-\upsilon)T_H(t-\rho-\upsilon) \\
& + p_2^{T_D/T_H} p_1^{T_H/T_D} q_2^{T_H/T_D} kT_D(t-\rho-\upsilon)T_H(t-\rho-\upsilon).
\end{aligned} \tag{4}$$

2.4 Cancer Cells

Being target cells, cancer cells, C, have similarly passive roles in the interactions as those of D and H, and thus the value of C represents the number

of cells in the base state and the two *Perish* states (i.e. all states other than *Death*). The state diagram for the cancer cells is given in Figure 5.

In addition, cancer multiplies at a logistic growth rate indicated by the closed loop at the top of the diagram. The logistic parameter r_C represents the net growth rate of cancer, which includes its natural death rate, and the parameter m_C represents the carrying capacity of the cancer population.

The C/T_H and C/T_C interactions are analogous to the T_D/D and the T_H/H interactions for the general blood cells in Section 2.1.

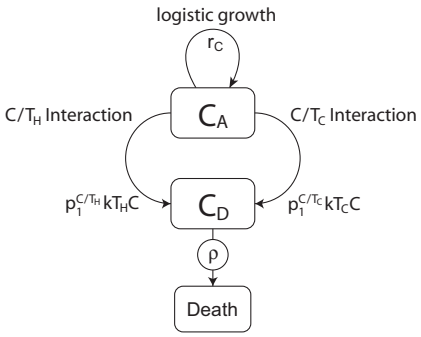

Fig. 5. Cancer diagram

The DDE for the evolution of C, that corresponds to Figure 5 is:

$$\begin{aligned}\frac{dC_A}{dt} &= r_C C(1-C/m_C) - p_1^{C/T_C} kCT_C - p_1^{C/T_H} kCT_H, \\ \frac{dC_D}{dt} &= p_1^{C/T_C} kCT_C + p_1^{C/T_H} kCT_H - p_1^{C/T_C} kC(t-\rho)T_C(t-\rho) \\ &\quad + p_1^{C/T_H} kC(t-\rho)T_H(t-\rho).\end{aligned} \tag{5}$$

2.5 Anti-Donor T Cells

The anti-donor T cells, T_D, respond to anti-cancer T cells T_C, general donor blood cells D, and anti-host T cells T_H the same way anti-host T cells respond to C, H, and T_D respectively. Hence, the diagram for anti-donor T cells is analogous to the one for anti-host T cells in Figure 4. This state diagram is given in Figure 6. The only difference is that we assume anti-cancer T cells cannot cause anergy in anti-donor T cells, so $q_3^{T_D/T_C} = 0$ on the lower right wing of Figure 6. Similarly, $q_3^{T_D/T_H} = 0$ on the lower left wing.

The DDE that corresponds to Figure 6 is:

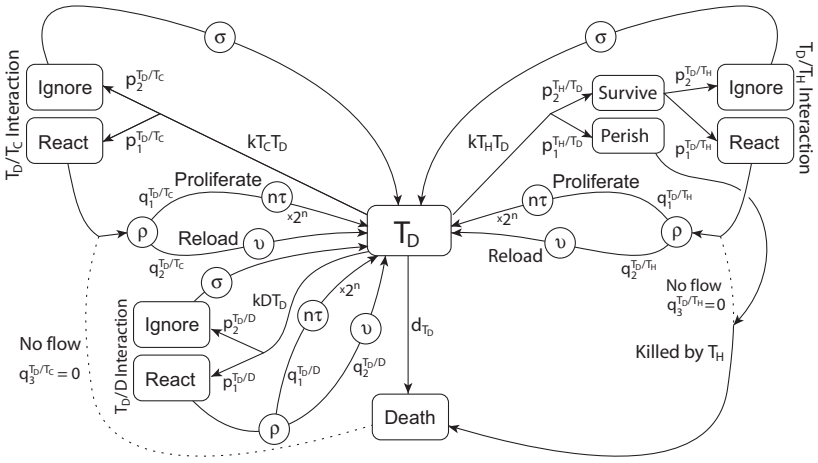

Fig. 6. Anti-donor T cell diagram

$$
\begin{aligned}
\frac{dT_D}{dt} = & -d_{T_D}T_D - kT_CT_D - kT_HT_D - kDT_D \\
& + p_2^{T_D/T_C}kT_C(t-\sigma)T_D(t-\sigma) \\
& + p_2^{T_H/T_D}p_2^{T_D/T_H}kT_H(t-\sigma)T_D(t-\sigma) \\
& + p_2^{T_D/D}kD(t-\sigma)T_D(t-\sigma) \\
& + 2^n p_1^{T_D/T_C}q_1^{T_D/T_C}kT_C(t-\rho-n\tau)T_D(t-\rho-n\tau) \\
& + 2^n p_2^{T_H/T_D}p_1^{T_D/T_H}q_1^{T_D/T_H}kT_H(t-\rho-n\tau)T_D(t-\rho-n\tau) \\
& + 2^n p_1^{T_D/D}q_1^{T_D/D}kD(t-\rho-n\tau)T_D(t-\rho-n\tau) \\
& + p_1^{T_D/T_C}q_2^{T_D/T_C}kT_C(t-\rho-\upsilon)T_D(t-\rho-\upsilon) \\
& + p_2^{T_H/T_D}p_1^{T_D/T_H}q_2^{T_D/T_H}kT_H(t-\rho-\upsilon)T_D(t-\rho-\upsilon) \\
& + p_1^{T_D/D}q_2^{T_D/D}kD(t-\rho-\upsilon)T_D(t-\rho-\upsilon).
\end{aligned}
\tag{6}
$$

3 Parameters

The various parameters and associated references used in our model are summarized in Table 1 and Table 2. Whenever possible, we obtained their values directly from the literature, although at times we had to make do with an estimation when specific information was unavailable. The initial concentrations and stem cell levels are summarized in Table 3. A detailed discussion of the parameters can be found in [1].

4 Numerical Simulations and Results

In delay differential equations, the values of the variables for $t < 0$ must be set as an initial condition. In our case, we handle this constraint by assuming that

Param.	Description	Estimate	References
Delays (day)			
ρ	Time for reactive T cell/ antigen interactions	0.0035 (5 min)	[4]
σ	Time for unreactive interactions	0.0007 (1 min)	[4]
τ	Time for cell division	$0.5 - 1.5$	[5, 6]
υ	T cell recovery time after killing another cell	1	[4]
Growth and Death Rates (day^{-1})			
d_{T_C}, d_{T_H}, d_{T_D}	T cell death rates	0.23	[7]
d_D, d_H	General death rate	0.1	Estimated
r_C	Net cancer growth rate	$10^{-3} - 10^{-2}$	[8, 3, 9]
m_C	Logistic carrying capacity for cancer	$1.5 - 3.5 \times 10^5$ (cells/μL)	Estimated
n	Avg # of T cell divisions after stimulation	< 8 times	[10]
Proportionality Constant for Mass Action $(\text{cells}/\mu\text{L})^{-1}\text{day}^{-1}$			
k	Kinetic mixing rate	10^{-3}	[11]

Table 1. Parameters

Param.	Description	Estimate
Probabilities		
$p_1^{X/Y}$	Prob. of a reactive X/Y interaction	$p_1^{X/Y} + p_2^{X/Y} = 1$
$p_2^{X/Y}$	Prob. of an unreactive X/Y interaction	
$q_1^{X/Y}$	Prob. that X proliferates after interaction	$q_1^{X/Y} + q_2^{X/Y} + q_3^{X/Y} = 1$
$q_2^{X/Y}$	Prob. that X keeps probing after interaction	
$q_3^{X/Y}$	Prob. that X becomes anergic after interaction	
$p_1^{T_H/H}$, $p_1^{T_H/T_D}$, $p_1^{T_D/D}$, $p_1^{T_D/T_C}$, $p_1^{T_D/T_H}$		0.9
$p_1^{T_C/C}$, $p_1^{T_H/C}$		0.8
p_1^{C/T_C}, p_1^{C/T_H}		0.6
$q_i^{T_H/H}$, $q_i^{T_H/T_D}$, $q_i^{T_D/D}$, $q_i^{T_D/T_C}$, $q_i^{T_D/T_H}$		0.5 $(i = 1, 2)$
$q_i^{T_C/C}$, $q_i^{T_H/C}$		0.25 $(i = 1, 2)$

Table 2. Transition Probabilities

Param.	Description	Estimate
Initial Concentrations (cells/μL)		
$T_C(0)$	Anti-cancer T cells	$10^{-1} - 1$
$T_H(0)$	Anti-host T cells	$10^{-1} - 1$
$D_A(0)$	General donor cells	$\leq 10^3$
$C_A(0)$	Cancer cells	$< 1.7 \times 10^{-3}$
$T_D(0)$	Anti-donor T cells	$\ll 1.7 \times 10^{-4}$
$H_A(0)$	General host cells	$\sim 10^3$
Stem Cell Supply Rates ((cells/μL) day^{-1})		
S_D	Donor cell resupply rate	$10^{-6} - 10^{-5}$
S_H	Host cell resupply rate	$10^{-8} - 10^{-7}$

Table 3. Initial Concentrations

the host cell populations are at a steady state before the transplant, while the donor-derived cell populations are not present until the time of the transplant (which is at $t = 0$). In other words, the values up to time 0 are denoted by the vector $[T_{C,0}\delta(t), T_{H,0}\delta(t), D_0\delta(t), C_0, T_{D,0}, H_0]$, where the terms $T_{C,0}$, $T_{H,0}$, D_0, C_0, $T_{D,0}$, and H_0 denote the concentrations of the six cell populations at time 0, and

$$\delta(t) = \begin{cases} 0 & \text{if } t \neq 0, \\ 1 & \text{if } t = 0. \end{cases}$$

In all our numerical simulations we use the 'dde23' delay-differential equation solver in MATLAB 6.5. The relative and absolute tolerances are left in their default values of 10^{-3} and 10^{-6}, respectively.

4.1 Parameter sensitivity analysis using LHS

In the original model of [1], we performed a sensitivity analysis that focused on two parameters at a time, i.e. we varried the values of two parameters while keeping all other parameters fixed. Using this approach we determined the relative importance of several parameters in determining the model behavior. Such a result from [1] is shown in Figure 1 which was obtained by varying the average number of T cell divisions per stimuation against the initial anti-host T cell concentration. In the model from [1], cancer populations could reach zero, and hence a successful outcome was defined as cancer elimination. An unsuccessful outcome was defined as the case where cancer relapses to over 1.5×10^5 cells/μL. An unresolved outcome as the case where neither scenario has occurred within 2000 days of transplantation.

Figure 1 suggests that higher initial anti-host T cell concentrations and higher average numbers of T cell division improve the chances of a successful outcome. In addition, the border line between the predominantly successful and the predominantly unsuccessful region is fairly clear.

To expand on the pairwise sensitivity analysis of [1] and to study the effects of all model parameters on the model behavior, we use Latin hypercube

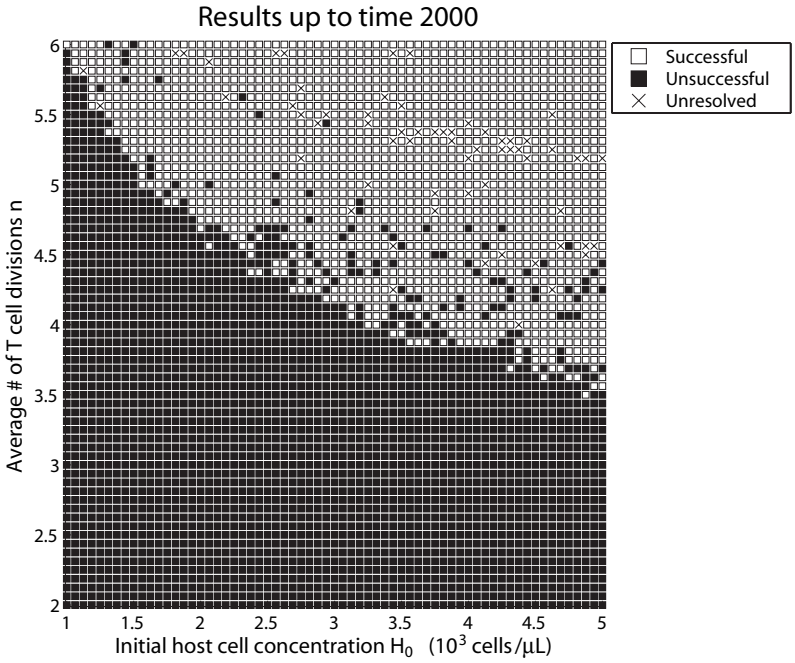

Fig. 1. Outcomes of model simulations with respect to the average number of T cell divisions per stimulation and the initial anti-host T cell oncentration.

sampling (LHS) [12]. This sensitivity analysis was not conducted for the model in [1]. such a study is useful for statistically determining which parameters are the most influential in affecting the outcome of the model's behavior.

LHS involves solving the system of equations multiple times with randomly sampled parameter values. The samples are chosen such that each parameter is distributed over its range of admissible values. We vary a wide range of parameters and measure their correlations to the minimum cancer concentration attained during the simulation and the time to the first cancer relapse. We define relapse as the time that the cancer population first recovers to 1000 cells/μL after its initial drop. Tables 1 and 2 show a list of varied parameters and correlations to the minimum cancer concentrations and relapse times, respectively.

Over the ranges that parameters were varied, the parameters that most strongly affect the minimum cancer concentration turn out to be the kinetic mixing coefficient k, the initial cancer concentration $C_A(0)$, and the initial host cell concentration $H_A(0)$. The most significant of the three is the initial host cell concentration. This observation implies that it is beneficial to preserve a high population of non-cancerous general host cells before the transplant. As

Param.	Description	PPMC	SROC	Range
ρ	Time for productive interaction	-0.0043	-0.0141	$0.0035 \pm 25\%$
σ	Time for nonproductive interaction	-0.0432	-0.0700	$0.0007 \pm 25\%$
τ	Time for one cell division	0.0358	0.0295	$1.0000 \pm 25\%$
υ	Time for T cell recovery after cytotoxic event	0.0053	-0.0002	$1.0000 \pm 25\%$
$p_1^{T_H/H}$	Prob. of anti-host T cell interaction with general host cell	-0.0664	-0.0722	$0.9 \pm 25\%$
$p_1^{T_C/C}$	Prob. of anti-cancer T cell interaction with cancer cell	0.0070	0.0282	$0.8 \pm 25\%$
p_1^{C/T_C}	Prob. of cancer cell interaction with anti-cancer T cell	-0.0339	-0.1427	$0.6 \pm 25\%$
$q_1^{T_H/H}$	Prob. that anti-host T cell divides after interaction	-0.2067	-0.2664	$0.5 \pm 25\%$
$q_1^{T_C/C}$	Prob. that anti-cancer T cell divides after interaction	-0.0836	-0.0633	$0.25 \pm 25\%$
d_{T_C}	Death rate of anti-cancer T cell	0.0818	0.1164	$0.1 \pm 25\%$
d_H	Death rate of host cell	0.0675	0.1320	$0.1 \pm 25\%$
r_C	Growth rate of cancer	0.0587	0.1106	0.01 to 0.05
m_C	Carrying capacity of cancer	-0.0135	0.0032	1 to 3×10^5
n_T	Average number of T cell divisions per stimulation	-0.2384	-0.3699	2 to 4
k	Kinetic mixing coefficient	**-0.3043**	**-0.3940**	0.5 to 2×10^{-3}
$C_A(0)$	Initial cancer concentration	**0.4082**	**0.2885**	0 to 1×10^{-2}
$T_C(0)$	Initial anti-cancer T cell conc.	-0.0813	-0.0770	0 to 10
$T_H(0)$	Initial anti-host T cell conc.	-0.1836	-0.2100	0 to 10
$T_D(0)$	Initial anti-donor T cell conc.	-0.0449	-0.0788	0 to 1×10^{-5}
$H_A(0)$	Initial host cell conc.	**-0.4858**	**-0.5892**	0 to 3000
$D_A(0)$	Initial donor cell conc.	-0.0208	-0.0436	0 to 1000
S_H	Stem cell supply rate of host cells	-0.0326	0.0273	0 to 1×10^{-6}
S_D	Stem cell supply rate of donor cells	-0.0505	-0.0530	0 to 1×10^{-4}

Table 1. Correlations between parameters (over the given ranges) and minimum cancer concentrations. Note that some parameters have a wider range than others. Correlation coefficients are as follows: Pearson product-moment correlation (PPMC), Spearman rank-order correlation (SROC)

discussed in [1], these general host cells provide stimulus to expand the T cells involved in the blood-restricted graft-versus-host immune response.

The two parameters that most strongly influence the relapse time are the cancer growth rate r_C and the initial host cell concentration. Clearly, if cancer grows faster, it will relapse faster. Hence, decreasing the cancer growth rate will have the strongest effect on slowing cancer relapse. This observation supports the conclusion of [3]. On the other hand, the initial host cell concentration remains significant for affecting cancer relapse. Hence, as an overall

Param.	Description	PPMC	SROC	Range
ρ	Time for productive interaction	0.0275	0.0190	$0.0035 \pm 25\%$
σ	Time for nonproductive interaction	0.0739	0.0951	$0.0007 \pm 25\%$
τ	Time for one cell division	0.0226	-0.0058	$1.0000 \pm 25\%$
υ	Time for T cell recovery after cytotoxic event	0.0219	-0.0095	$1.0000 \pm 25\%$
$p_1^{T_H/H}$	Prob. of anti-host T cell interaction with general host cell	0.0283	0.0120	$0.9 \pm 25\%$
$p_1^{T_C/C}$	Prob. of anti-cancer T cell interaction with cancer cell	-0.0805	-0.0479	$0.8 \pm 25\%$
p_1^{C/T_C}	Prob. of cancer cell interaction with anti-cancer T cell	0.1345	0.1398	$0.6 \pm 25\%$
$q_1^{T_H/H}$	Prob. that anti-host T cell divides after interaction	0.1094	0.1148	$0.5 \pm 25\%$
$q_1^{T_C/C}$	Prob. that anti-cancer T cell divides after interaction	-0.0246	-0.0139	$0.25 \pm 25\%$
d_{T_C}	Death rate of anti-cancer T cell	-0.0416	-0.0495	$0.1 \pm 25\%$
d_H	Death rate of host cell	-0.1142	-0.0849	$0.1 \pm 25\%$
r_C	Growth rate of cancer	**-0.8072**	**-0.8691**	0.01 to 0.05
m_C	Carrying capacity of cancer	0.0378	0.0505	1 to 3×10^5
n_T	Average number of T cell divisions per stimulation	0.1771	0.1792	2 to 4
k	Kinetic mixing coefficient	0.1818	0.1936	0.5 to 2×10^{-3}
$C_A(0)$	Initial cancer concentration	-0.1061	-0.1171	0 to 1×10^{-2}
$T_C(0)$	Initial anti-cancer T cell conc.	0.0997	0.0766	0 to 10
$T_H(0)$	Initial anti-host T cell conc.	0.0814	0.0878	0 to 10
$T_D(0)$	Initial anti-donor T cell conc.	0.0802	0.0728	0 to 1×10^{-5}
$H_A(0)$	Initial host cell conc.	**0.3160**	**0.3446**	0 to 3000
$D_A(0)$	Initial donor cell conc.	0.0623	0.0678	0 to 1000
S_H	Stem cell supply rate of host cells	-0.0137	0.0082	0 to 1×10^{-6}
S_D	Stem cell supply rate of donor cells	0.0497	0.0488	0 to 1×10^{-4}

Table 2. Correlations between parameters (over the given ranges) and the time to cancer relapse. We define the time of relapse to be the time that the total cancer concentration recovers to over 1000 cells/μL.

strategy, it might be more effective to preserve as many general host cells as possible prior to transplantation.

4.2 Simulating initial conditions of minitransplants

The most natural way to preserve a high host cell population is to reduce the level of chemotherapy. However, reduced chemotherapy also leads to higher leukemia loads before transplantation. Transplants performed under reduced chemotherapy are called non-myeloablative, or mini-, transplants. In mini-

transplants higher levels of both the general host cell and cancer cell populations are retained.

We apply the model to study the influences of these two populations on the success of the transplant. Since the model is based on a system of deterministic differential equations, the cancer population never attains a 0 value. (See Figure 2 for an example of the time evolution of cancer, T cell, and general host cell populations.) Instead, we say that the cancer population is eliminated if its concentration passes below the concentration of one cell in the body. (We estimate this concentration to be around 1 cell/6L of blood $\sim 10^{-7}$ cells/μL.) We say that a transplant is successful if this threshold is crossed and refer to this barrier as our extinction criterion.

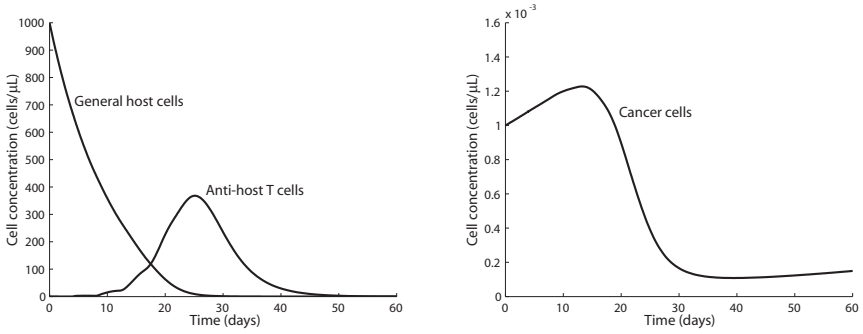

Fig. 2. Time evolution of general host cell, anti-host T cell, and cancer cell populations. Because cells, die at a proportional rate, the cancer cell population may become very low, but it never reaches zero. Hence, the cancer population always eventually relapses. Parameter values are given in the appendix

Using the model and applying the extinction criterion, we obtained preliminary results showing how a transplant's success depends on the two parameters: the initial (non-leukemic) host cell concentration and the initial leukemia concentration. Using LHS, we randomly varied these two parameters uniformly between 0 and 3000 cells/μL and logarithmically between 10^{-3} and 10^{3} cells/μL, respectively. To obtain a more diverse sample, we simultaneously varied the other model parameters within a range of $\pm 25\%$ of their estimated values.

The results are shown in Figure 3. The x-axes show the initial cancer cell concentrations on a log scale, and the y-axes show the initial (non-leukemic) host cell concentrations. Figure 3(top) simply shows in black and white when cancer cells were eliminated (by the extinction criterion) and when they survived. Figure 3(bottom) shows the same plot in a grayscale, where black indicates a minimum cancer concentration at or below 10^{-7} cells/μL (extinction

level) and white indicates a minimum cancer concentration at or above 10^{-2} cells/μL.

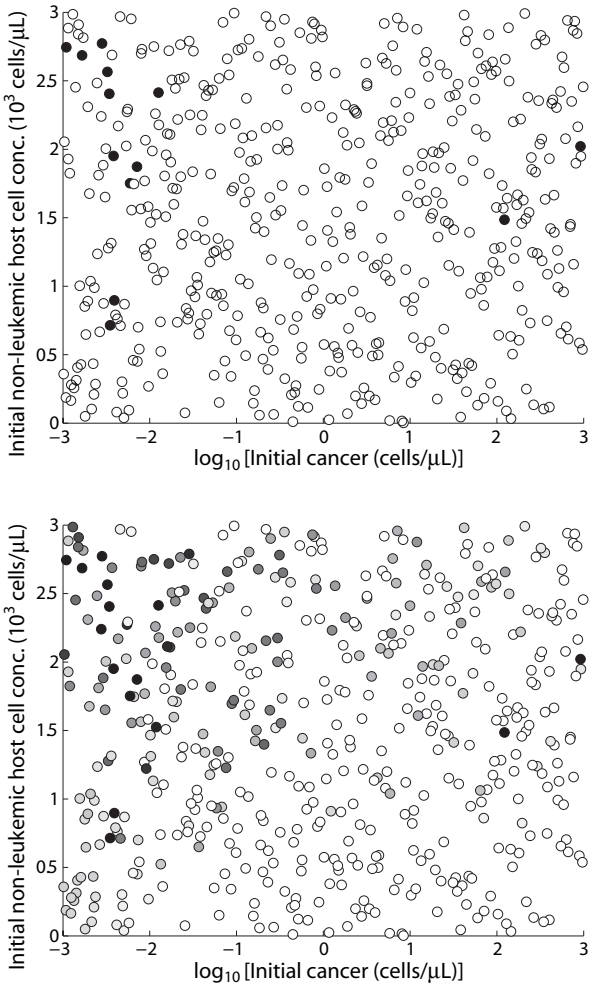

Fig. 3. Scatter plots of transplant outcomes with respect to initial non-leukemic host cell concentrations and cancer cell concentrations. All model parameters are varied using Latin Hypercube Sampling. *Top*: Black indicates cancer elimination, and white indicates cancer relapse. *Bottom*: Grayscale plot where the shade corresponds to the minimum cancer concentration attained after transplant. Black indicates complete elimination. White indicates a minimum cancer concentration of greater than 10^{-2} cells/μL

As expected, the figures show that it is best to start with almost no leukemia cells and as many non-leukemic host cells as possible. This ideal, however, is not always possible. The figures also show that having very little non-leukemic host cells makes it almost impossible to eliminate cancer, regardless of the initial cancer concentration. In addition, Figure 3(bottom) shows that the anti-leukemia immune response might do better even against a high level of cancer cells, if it has sufficient stimulus from non-leukemic cells. Our goal in this study is to determine ideal conditions for a successful transplant and devise treatment strategies to get as close to this ideal as possible. In some cases, mini-transplants might be more effective than full transplants, especially in cases where full transplantations are risky.

5 Discussion

In this paper, we extended the model of [1] by dividing all target cells into two states: alive and dying. This modification accounts for the delay between the time that a T cell engages a target cell and the time that the target cell actually dies. During this time period, target cells may continue to stimulate other circulating T cells.

Our analysis of the parameter sensitivity indicates that the initial host cell concentration is the most important parameter in influencing the minimum cancer concentration and the cancer relapse time together. A low minimum cancer concentration most likely implies that there is a higher probability that the cancer population was completely eliminated. This analysis supports the conclusion on [1]. Alternatively, a low cancer growth rate hardly affects the minimum cancer concentration, but strongly affects the relapse time. This last result supports the conclusion of the analogous CML model, based on ordinary differential equations, of [3].

We also use Latin hypercube sampling to examine the affects of the initial host cell and cancer cell concentrations on the outcome of a transplant. Our simulations show that it may be advantageous to attempt to decrease a host's cancer load while sparing as many general host cells as possible. Not only will this approach lead to a less toxic treatment before transplantation, but it will also improve the effectiveness of the donor-derived graft-versus-host immune response.

As a future work, we plan to conduct a more thorough analysis of the dynamics of minitransplants. Various strategies to minimize a patient's leukemia load, while preserving a supply of non-leukemic host cells are to optimally lessen the dosage of chemotherapy, administer the drug Gleevec to selectively inhibit cancer proliferation, or to use both methods in cominbination. With modeling, we intend to gain insights into the most effective combination of pre-transplant therapies. We will also consider whether certain post-transplant therapies such as donor lymphocyte infusion or cancer vaccination may enhance the effectivenes of the treatment.

Acknowledgments: The work of Doron Levy was supported in part by the NSF under Career Grant DMS-0133511. The work of Peter S. Kim was supported by the NSF Graduate Research Fellowship Program and the Department of Mathematics at Stanford University. The work of Peter P. Lee was supported by a Research Scholar Award from the American Cancer Society. We would also like to acknowledge the Blood and Marrow Transplantation Division of the Stanford Medical School for providing us with parameters derived from CML patients who underwent allogenic bone marrow transplantation.

References

1. DeConde, R, Kim, P. S, Levy, D, & Lee, P. P. (2005) *J Theor Biol.* **236**, 39–59.
2. Schiffer, C. A, Hehlmann, R, & Larson, R. (2003) *Leukemia* **17**, 691–699.
3. Moore, H & Li, N. K. (2004) *J Theor Biol.* **225**, 513–523.
4. Friedl, P & Gunzer, M. (2001) *Trends Immunol.* **22**, 187–191.
5. Chao, D. L, Forrest, S, Davenport, M. P, & Perelson, A. S. (2003) *Proc IEEE Comput Soc Bioinform Conf.* **2**, 124–131.
6. Lee, P. P. (2007). Unpublished data: generated by the Lee Lab at Stanford Medical School.
7. Duvall, C. P & Perry, S. (1968) *J Lab Clin Med.* **71**, 614–628.
8. Fokas, A. S, Keller, J. B, & Clarkson, B. D. (1991) *Cancer Res.* **51**, 2084–2091.
9. Stryckmans, P. A, Debusscher, L, & Collard, E. (1977) *Clin Haematol.* **6**, 21–40.
10. Antia, R, Bergstrom, C. T, Pilyugin, S. S, Kaech, S. M, & Ahmed, R. (2003) *J Theor Biol.* **221**, 585–598.
11. Luzyanina, T, Engelborghs, K, Ehl, S, Klenerman, P, & Bocharov, G. (2004) *Math Biosci.* **173**, 1–23.
12. McKay, M. D, Conover, W. J, & Beckman, R. J. (1979) *Technometrics* **21**, 239–245.

A Parameters for figures

Parameter	Value		
Figure #	1	2	3
ρ	0.0035	0.0035	0.0035
σ	0.0007	0.0007	0.0007
τ	1	1	1
υ	1	1	1
$p_1^{T_H/H}$, $p_1^{T_H/T_D}$, $p_1^{T_D/D}$, $p_1^{T_D/T_C}$, $p_1^{T_D/T_H}$	0.9	0.9	0.9
$p_1^{T_C/C}$, $p_1^{T_H/C}$	0.8	0.8	0.8
p_1^{C/T_C}, p_1^{C/T_H}	0.6	0.6	0.6
$q_1^{T_H/H}$, $q_1^{T_H/T_D}$, $q_1^{T_D/D}$, $q_1^{T_D/T_C}$, $q_1^{T_D/T_H}$	0.5	0.5	0.5
$q_2^{T_H/H}$, $q_2^{T_H/T_D}$, $q_2^{T_D/D}$, $q_2^{T_D/T_C}$, $q_2^{T_D/T_H}$	0.5	0.5	0.5
$q_1^{T_C/C}$, $q_1^{T_H/C}$,	0.25	0.25	0.25
$q_2^{T_C/C}$, $q_2^{T_H/C}$	0.25	0.25	0.25
d_{T_C}, d_{T_H}, d_{T_D}	0.23	0.23	0.23
d_D, d_H	0.1	0.1	0.1
r_C	0.02	0.02	0.02
m_C	2×10^5	2×10^5	2×10^5
n	2 to 6	4	
k	0.001	0.001	0.001
$T_{C,0}$	1	0	0
$T_{H,0}$	1	1	1
D_0	1000	0	0
C_0	0.001	0.001	10^{-3} to 10^3
$T_{D,0}$	10^{-5}	0	0
H_0	1000 to 5000	1000	0 to 3000
S_D	10^{-5}	10^{-5}	10^{-5}
S_H	10^{-7}	10^{-7}	10^{-7}